1. Introduction

1.1 The concept of nanocomposites

In recent years, scientists and engineers have developed the ability to exploit the nanometric (10^{-9} m) dimension of materials, bringing revolutionary breakthroughs in such fields as materials science, electronic and optical engineering, catalytic chemistry and biological applications. The field of nanocomposites is a special subset of these from an economic point of view, due to their top-down manufacture. In theory, they can be mass produced at a price comparable to standard composite materials. The difference between nanocomposites and traditional composite materials is that, in the former, the particle diameters are of the order of 10 nm, whereas in the latter they exceed 1 μm. Another difference is that the filler loading level required to obtain acceptable nanocomposite performance is typically an order of magnitude smaller than a functionally comparable microcomposite.

Nanocomposites are, as an extension to the field of materials science, the execution of a concept already perfected in nature. Ball [1.1], in discussing the nanoscale systems found in nature for biomimetic applications, notes that even the materials that make up our bodies are nanostructured. For example, the properties of bone are not simply a mixture of inorganic and organic constituents, but rather depend critically on the structural properties of the material at various levels of organisation. Technologically, the development of polymer nanocomposites can be thought of as the next logical step in the history of modern synthetic polymer composites, which began in the 1900s with the use of wood flour-filled polymers for improved heat resistance, minimised shrinkage and reduced cost [1.2].

In fact, the technology for the manufacture of some nanocomposites, if not the scientific understanding, was known by the ancients. The Lycurgus cup, dating from the 4th century AD, appears green in reflected light and red in transmitted light due to the incorporation of gold/silver alloy nanoparticles within the glass matrix [1.3]. Nano-gold, which has been used for hundreds of years to colour church windows, was studied in its colloidal form by Faraday in

the 19th century [1.4]. Other examples of pre-modern nanocomposite technology are the Damascus swords, whose remarkable mechanical properties are the result of cemenite nanowires and carbon nanotubes within the metallic matrix of the blade [1.5].

As discussed by Lewis [1.6] the effect of nanostructuration can be thought in terms either of increased specific interfacial area or of decreased inter-particle distance. From a dielectric point of view, the former property would be expected to affect the polarisation properties of a material, the latter the charge transport processes. If we imagine a composite material with a uniform distribution of spherical filler particles, the distance between any two particles will be a constant fraction of the particle diameter, whereas the specific interfacial area will relate to the particle diameter in linear inverse proportion. Furthermore, provided agglomeration can be prevented, the nanocomposite case will more accurately fit such a uniform distribution approximation.

One must also pay close attention to the interfacial regions associated with the particle surface, where interactions between the filler and the matrix give rise to a tertiary region whose physical properties differ from both phases. If the characteristic width of this region is ~10 nm [6], it follows that the volume fraction of this region in many nanocomposites can be close to 100%. Tanaka elaborates on the ideas due to Lewis with a multi-core model comprising a spherical nanoparticle surrounded by an interface region between the nanoparticle and the surrounding polymer [1.7]. Outside this region, the polymer cannot “see” the nanoparticle.

Tanaka’s interface consists of 3 layers. The first layer consists of those chains that are tightly bound to the nanoparticle. The second layer consists of chains that interact strongly with the first layer and so are more tightly bound than the matrix. The third layer, however, is loosely bound and has a *higher* free volume than the matrix due to surface tension effects between the second layer and the bulk matrix. There is also a double layer of electric charge superimposed on all three regions to form a dipole moment. It is principally the second and third layers that govern the electrical characteristics, and the relative volume fractions of these layers vary from nanocomposite to nanocomposite. It is better to call this a paradigm than a

model, since it has little predictive power. Provided this distinction is borne in mind, its usefulness can be appreciated. The tightly bound second layer is capable of describing increases in mechanical strength, electrical erosion resistance and permittivity, together with reduced molecular mobility and corresponding increases in glass transition temperature. Conversely, *reductions* in glass transition temperature and permittivity can be thought of in terms of a dominant third layer. This situation, where the non-existence of the second layer is inferred, could correspond to the case where the filler is well dispersed but remains thermodynamically incompatible with the matrix. Alternatively, in epoxy systems, it is conceivable that the hardener might be scavenged by the filler particles, leading to a matrix which is not stoichiometrically crosslinked. Tanaka considers the enhanced mobility observed in some nanocomposites in terms of a shallower trap distribution in the third region.

Composite polymers have various uses in the electrical power industry. For example, hydrated alumina is used extensively in outdoor insulation applications to provide flame retardancy and tracking resistance [1.8]. The conducting properties of carbon black are exploited in cable insulation for field grading [1.9]. If mechanical reinforcement is required for load-bearing members in substations, high purity fillers such as pyrogenic silica can be used [1.2]. However, using polymer composites in the electrical power industry generally involves much compromise. For example, the two commercially-available grades of fibre glass are named E-glass and S-glass for their electrical and structural suitability respectively [1.10]. As discussed in Chapter 7, the incorporation of micron-sized fillers into polymeric insulation rarely improves the electrical breakdown strength, and is often detrimental to it. Against this background, it is hoped that well-designed nanocomposite dielectrics might provide improved all-round electrical, mechanical and thermal properties without compromises having to be made.

Particularly promising are materials that offer greater resistance against electrical erosion. El-Hag *et al.* [1.11] compared the laser ablation resistance of silicone rubber filled with 12 nm fumed silica particles with the same matrix filled with 5 μm silica. Laser ablation is a controllable way of locally reproducing the kind of temperatures likely to be experienced by material

surfaces during dry-band arcing. They found that a 5% loading of nanofiller resulted in less eroded mass than did 30% of microfiller, as illustrated in Figure 1.1 below. The reason for improved erosion resistance was shown to be the formation of a silica-rich protective barrier on the surface, whereupon the material was behaving in a manner comparable to nanocomposite systems that exhibit superior flame resistance [1.12]. Kozako *et al.* [1.13] drew attention to the crystallisation of polyamide spherulites on layered synthetic mica, resulting in partial discharge-resistant "stair-like" structures forming out of less resistant amorphous regions. Conversely, Sarathi *et al.* [1.14] remark that well-exfoliated clay structures can act as oxygen barriers to inhibit bulk degradation, a phenomenon that is being developed for exploitation in the food packaging industry.

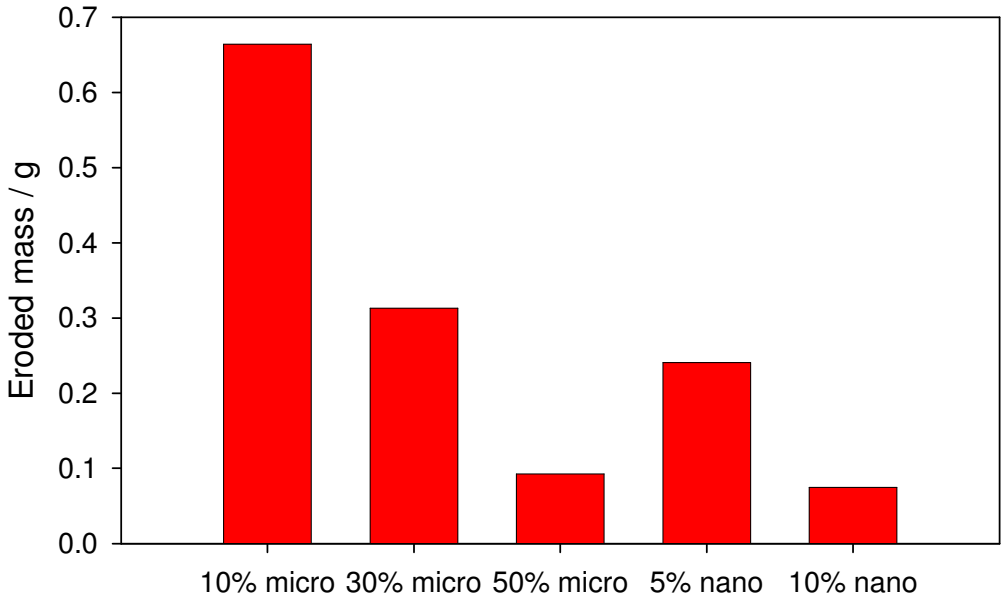

Figure 1.1: Comparative laser ablation resistance of nano- and micro-filled silicone rubber, reproduced from [1.7].

1.2 The filler: montmorillonite clay

This research studies systems composed of polyethylene filled with montmorillonite (MMT) clay. Table I, reproduced from Tanaka *et al.* [1.7] summarises the properties of nanocomposites produced from MMT in various polymer matrices. Note that the electrical properties are especially uncertain.

Property	Change in properties due to nanostructuration
1. Mechanical: (a) Tensile strength	Improved (1.5 – 3 times)
(b) Elongation at break	Much decreased (<10%)
(c) Bending strength	Improved (1.5 – 3 times)
(d) Elastic modulus	Improved (2 – 4 times)
(e) Impact strength	Marginal difference/slightly decreased
(f) Tribology (frictional properties)	Improved
(g) Creep and fatigue	Improved
2. Thermal (a) Temperature of deflection under load	Improved (by over 80 ℃ for crystalline polymers, 20-30 ℃ for amorphous polymers.)
(b) Melting point	Negligible difference
(c) Heat decomposition temp	Improved
(d) Expansion coefficient	Decreased (by 50%)
(e) Thermal conductivity	Theoretical improvement
(f) Glass transition temperature	Theoretical Improvement
3. Other (a) Weathering resistance	Not distinct
(b) Chemical resistance	Unchanged
(c) Transparency	Unchanged, improved in some crystalline polymers
(d) Water absorption	Improved

(e) Size stability	Improved
(f) Specific gravity	Almost unchanged
4. Functional (a) Barrier performance	Improved (2-10 times)
(b) Flame retardancy	Improved (especially reduction in heat generation rate)
(c) Biodegradability	Not distinct (accelerated in some cases.)
(e) Paint performance	Surface hardness, weathering resistance etc improved
5. Electrical (a) Partial discharge and tracking resistance	Improved
(b) DC conductivity	Complex results
(c) Space charge	Complex results
(d) Interfacial polarisation	Reduced
(e) Permittivity	Complex results

Table 1.1: Summary of properties of MMT/polymer nanocomposites compared to virgin polymer (reproduced from Tanaka [1.7].)

The structure of MMT is given in Figure 1.2. Each layer consists of an octahedral sheet of alumina sandwiched between two tetrahedral sheets of silica. The layers are separated by a "gallery" and are only loosely bound by Van der Waals forces. Substitution of an aluminium ion for one of lower valency such as sodium or magnesium results in the layers becoming positively charged, this charge being balanced by ions in the interlayer spacing. The extent of this phenomenon is measured by the so-called "cation exchange capacity." As a result of this, the clay is strongly hydrophilic and will not readily disperse in non-polar polymers such as polyethylene.

In order to render montmorillonite compatible with a non-polar polymer, one must address the polarity issue. Either the polymer must be rendered more polar or the clay must be made more organophilic (or both.)

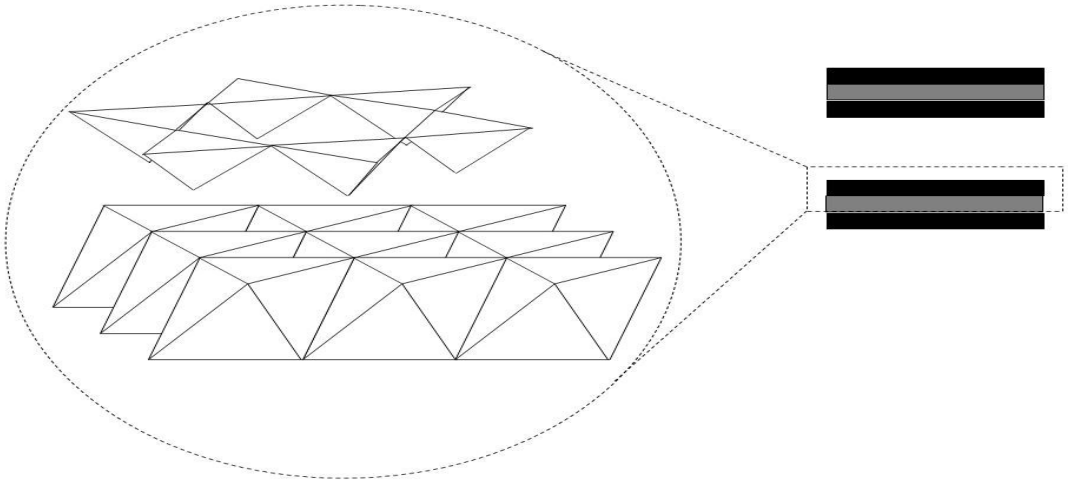

Figure 1.2: Crystal structure of two thirds of a phyllosilicate layer. Oxygen atoms are located on the corners of the octahedra and tetrahedra. The octahedral and tetrahedral layers are touching, but shown "exploded" for clarity. An OH^- ion is situated at the corner of the octahedra underneath the "hole" in the tetrahedral ring. To complete the phyllosilicate layer, add another silicate layer underneath the alumina layer. This structure, comprising an octahedral layer sandwiched between two tetrahedral layers is known as a "2:1 phyllosilicate."

The latter is the more established technique, and is achieved by adding cationic surfactants such as alkylphosphonium or, in this work, alkylammonium ions between the layers.

There are 5 conceptual phases that can exist when MMT is dispersed in PE by mechanical melt mixing, as described by Dennis *et al* [1.15]. Melt mixing is the most feasible method for large-scale MMT nanocomposite preparation as it requires only a little modification of existing melt-blending equipment. The clay starts off as aggregates (0.1-1 mm,) before breaking up into firstly primary particles (1-10 μm,) then tactoids (0.05-0.5 μm.) These initial phases are easily achievable and are trivial, producing micro- rather than nanocomposites. The next stage of thermodynamic difficulty is when polymer chains enter into the galleries and the interlayer spacing increases. This is known as intercalation, and the associated increase in interlayer distance is easily detected using X-ray diffraction. The final level of

thermodynamic difficulty is exfoliation, where the clay nanolayers are separated from each other and dispersed randomly in the polymer matrix. The final 3 states are illustrated schematically in Figure 1.3.

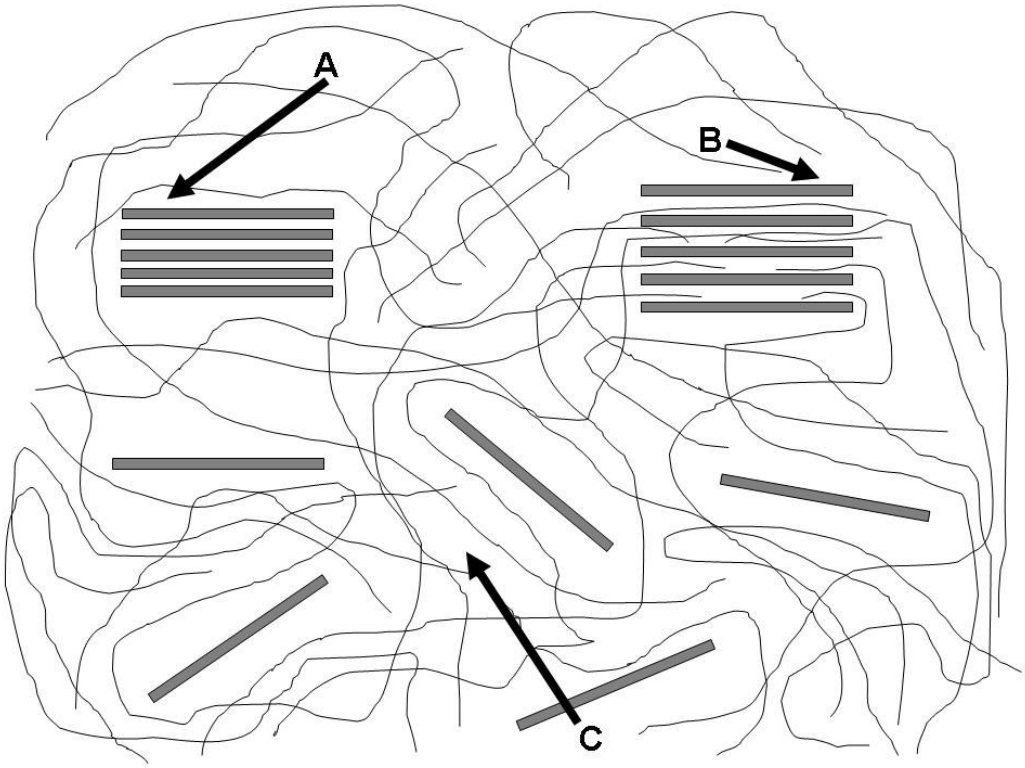

Figure 1.3: MMT platelets in various degrees of dispersion. (A) phase-separated, (B) intercalated, (C) exfoliated.

Work on the thermodynamics of melt intercalation [1.16],[1.17],[1.18] has shown that the behaviour of the alkyl chains in the galleries is critical. An increase in the length of the surfactant chains increases the interlayer separation, making intercalation easier. The loss in entropy caused by the confinement of polymer chains during intercalation is balanced by the freedom gained by the alkyl chains, and so long as the enthalpic considerations are favourable, intercalation and perhaps exfoliation will take place.

Other methods of preparing MMT nanocomposites include in-situ polymerisation of a monomer in which the clay has been swollen, exfoliation-adsorption, in which the clay and the polymer are together dissolved in a

solvent and then precipitated to form an ordered structure, and template synthesis, where the silicates themselves are formed in situ in an aqueous solution of the polymer and the components of the silicates. They are reviewed by Oriakhi [1.19], but are not of interest for this study.

1.3 The matrix: polyethylene

Polyethylene is a semicrystalline polymer, comprising crystalline regions in an amorphous matrix. Individual crystals take the form of lamellae, which are sheets containing parallel chain portions. Their dimensions are typically a few nanometres parallel to the chains and up to a micron in the directions perpendicular to them (along the sheet.) It had been thought, according to the "fringed micelle" model, that each chain passed through a lamella only once, so that crystalline regions were no more than local, ordered groupings of chains. However, work undertaken especially by Keller [1.20] demonstrated that lamellae are in fact composed of chains which repeatedly fold back on themselves. Chains that do not fold back into a lamella upon reaching its surface of folded chains are free to enter another lamella, re-enter the original lamella at a different point or just remain in the amorphous region. This is illustrated in Figure 1.4 (A). A typical value of the proportion of chains that undergo adjacent re-entry is 75%, as determined by Spells [1.21] in infra-red spectroscopy of single PE crystals grown from solution.

Due to molecular conformations, polyethylene chains inside a lamella are not in fact perpendicular – Figure 1.4(A) is drawn as such for clarity – rather there is a 30° tilt which is best observed when single polyethylene crystals are grown from solution as pyramids.

Gedde [1.22] shows that for a 6-sided right-angled crystal in equilibrium, the ratios of the free energies of each surface to the thickness of the crystal perpendicular to each surface should be equal. In PE lamellae, this is not the case, and so there is considerable thermodynamic drive for them to thicken upon annealing. Impurities and chain branching are deleterious to lamellar thickness as they are not readily incorporated into crystals.

Polyethylene also exhibits several supercrystalline structures. These range from fibrillar structures in highly-drawn materials (or materials with

fibrous fillers such as dibenzylsorbitol,) through to sheaves of lamellae at high temperatures. The most common superstructure is the spherulite (Greek for “little sphere.”) This is illustrated in Figure 1.4 (B). These are spherically symmetric objects formed when a few lamellae form together at a nucleus and grow outwards. As they do so, the lamellae splay and diverge, filling out the available space to give a spherical envelope.

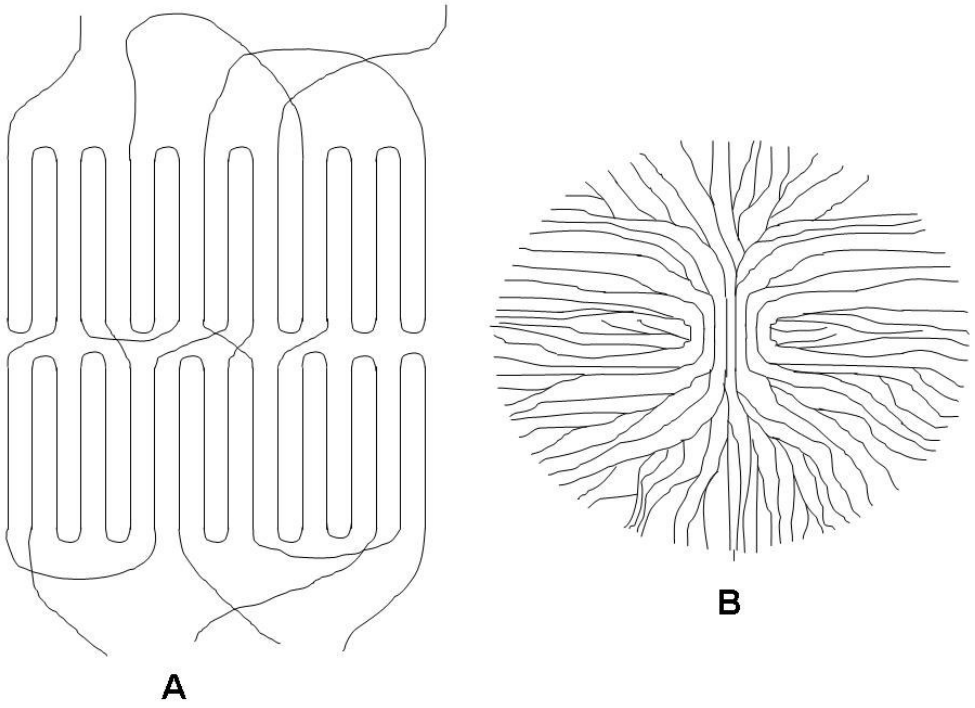

Figure 1.4 (A) A stack of two lamellae with interconnecting polymer chains. (B) Schematic of a spherulite.

Spherulites can be viewed using polarised light microscopy by exploiting the phenomenon of birefringence. They exhibit a Maltese-cross pattern of extinction (darkness) corresponding to planes parallel to both the polariser and analyser. When formed at high degrees of supercooling, they are known as “banded” because they display alternating bands of light and dark as the refractive index ellipse rotates around the radius of the spherulite.

Until recently, the most popular mechanism for spherulite growth was that of Keith and Padden [1.23]. The theory purported to explain the spherical symmetry and fibrosity observed by considering the rejection of impurities and uncrystallisable material from lamellar growth fronts. Ejected material will lower the effective degree of supercooling at the front, reducing the thermodynamic drive for growth. Protuberances, however, can break free from this impasse, causing a spreading of fibres, eventually achieving spherical symmetry. It is pointed out by Vaughan [1.24] that "fibrous" is a rather misleading and unfortunate word – in the language of Keith and Padden, it refers to the actual formation of fibres due to lamellar habit degeneration, which does not happen. The fibrous texture of a spherulite is instead a consequence of the angular distribution of dominant and subsidiary (infilling) lamellae.

Work at Reading University in the late 1970s / early 1980s under the direction of Bassett [1.25] has successfully challenged the validity of this model. It is recognised now that lamellar splaying is in fact caused by screw dislocations, followed by separation due to interference of interlamellar cilia (chain ends.) This may or may not be associated with banding. Bassett notes that, for polyethylene, lamellae which are formed at large degrees of undercooling result in irregular fold surfaces as new layers of chains nucleate before previous layers have had time to complete and order themselves. Subsequent reordering of the fold surface distorts the lamella into an S or C-shape. When these lamellae pack together, this phenomenon becomes the driving force for regular, frequent, isochiral screw dislocations which cause banding. The driving force is not an elastic strain but a geometrical requirement. This explains why banded growth does not happen above ~120 ^{0}C in polyethylene – too much time exists for molecular reordering effects.

1.4 Dielectric breakdown of polymers

The electric stress which a polymeric insulator is able to withstand may be a function of charge transport, thermal and mechanical effects, and a fully comprehensive picture can only be obtained by considering all of these. The

earliest breakdown theories treated breakdown events as arising from thermal instabilities. Such instabilities could be in the steady-state power balance between electrical heating and Newtonian cooling, or they could exist intrinsically as a positive feedback process between temperature and conductivity [1.26]. Garton and Stark [1.27] proposed a mechanical model, where a metastable balance exists between the electrostrictive force provided by the electrodes and the compressive reaction force of the sample: the breakdown strength was therefore considered as a function of the Young's modulus of the material.

These earlier, cruder models eventually evolved into more sophisticated filamentary thermal and mechanical models. The most advanced filamentary mechanical models are those due to Zeller and Schneider [1.28] and Fothergill [1.29]. These are used to model the growth of electrical trees. A crack will propagate when the energy required to create the crack is less than the strain energy liberated by the cracked material. The models differ in the physical parameters they use, the former using surface tension and yield strength; the latter, fracture toughness and Young's modulus. More recently, Zebouchi and Malec have published numerical solutions to a combined thermal and mechanical breakdown model (not a filamentary type) [1.30]. They attribute the remaining discrepancies in the data for polyethylene terephthalate (PET) films to the presence of space charge.

In the vast majority of cases, discernment between the various breakdown mechanisms is difficult, if not impossible. Ieda [1.31] reviews research on a range of polymers, noting that the strong variation of breakdown strength with temperature at high temperatures is well suited to the thermo-mechanical models. He argues that at low temperatures (below 30 ℃ for polyethylene,) constant breakdown strengths imply an electronic breakdown mechanism. Dissado and Fothergill make the case that the data are also consistent with an electromechanical breakdown mechanism under a constant, high value of Young's modulus [1.32].

Concerning electronic breakdown theories, O'Dwyer [1.33] distinguishes between avalanche breakdown, where a positive feedback mechanism exists in the density of free carriers due to impact ionisation, and energetic theories. In these, a power balance equation can be constructed in

terms of the energy gained from the field and the energy lost to the material through electron collisions. The simplest consideration is the Von Hippel criterion [1.34], which considers the energetics of a uniform distribution of electron energies. Fröhlich [1.35] added more power to the model by treating the electron energy distribution as non-uniform, thereby predicting lower, more realistic breakdown strengths. In all of these cases, the ultimate breakdown event is an unstable current, which destroys the sample by melting. Alternatively, the scattering process can be considered as a potential source of chain scisson in free volume regions. This idea, originally due to Artbauer, was developed in the 1980s by Nelson and Sabuni, who noted the correlation between the breakdown strengths of some polymers with their glass transition temperatures and cohesive energy densities [1.36].

A helpful concept when discussing charge transport in polymers is that of the trap distribution. Traps, which are electron-localising potential wells, can be classified as “deep” or “shallow.” Deeply trapped electrons are those which are too immobile to take part in conduction; they are responsible for the storage of space charge. As the depth of the potential well decreases, there is an increase in trap density, leading to the concept of the “mobility edge,” above which the traps are classified as “shallow,” and the electrons can take part in the conduction process. The energy of the trapped electron will be of the form:

$$P(E) \propto \exp\left(\frac{E - E_{\min}}{k_B T}\right) \tag{1.1}$$

where *P(E)* is the probability that the electron has an energy *E*, *T* is the temperature in Kelvin and k_B is the Boltzmann constant. At a given temperature, there will be a certain number of electrons that are able to hop over the energy barriers into neighbouring traps; an externally applied field will impose a potential gradient on the trap distribution, making hops in the direction of the field more likely than against the field. Dissado and Fothergill [1.32] argue that this scenario is unlikely in polymers, as the barriers are too

high. Inter-state tunnelling is more likely to occur, whereby electron wavefunctions are delocalised across neighbouring traps.

If the electron energies are high enough, the electron mobilities become limited by scattering processes rather than trap distributions (although the traps may nonetheless serve as scattering centres.) Teyssedre and Laurent [1.37] discuss some complexities pertaining to this situation. Firstly, in the case of extended crystalline structures, conduction and valence bands have been derived from *ab initio* density functional theory (DFT) in order to interpret data from X-ray photoelectron spectroscopy (XPS) experiments. This implies that in these situations, energetic electrons can be considered as moving as delocalised waves in a conduction band – perhaps with holes in the valence band. It is important to remember, though, that holes cannot exist in the amorphous regions, where the valence electrons must be localised in the tightly-bound covalent bonds. Ultimately, the charge transport dynamics of the high field, high temperature case are likely to be space charge limited. The simplest treatment of this is due to Mott and Gurney [38], where for an infinite slab:

$$J = \frac{9\varepsilon_0 \varepsilon_r \mu V^2}{8s^3} \tag{1.2}$$

where J is the current density, V the applied voltage, μ the electron mobility, s the thickness and $\varepsilon_0\varepsilon_r$ the dielectric permittivity.

Recent discussions of charge transport and breakdown processes in polymers have emphasised the importance of taking into account morphological considerations, stressing the fact that at a microscopic level, electronic and mechanical considerations may not be so distinct after all. Lewis [1.39] discusses the application of the Helmholtz equation at the microscopic level:

$$\overline{F} = \rho\overline{E} - \frac{1}{2}E^2\nabla\varepsilon + \frac{1}{2}\nabla\left(\rho_m \frac{\partial \varepsilon E^2}{\partial \rho_m}\right) \tag{1.3}$$

where E and F are the local electric field and corresponding mechanical stress respectively, and ρ and ρ_m are the charge and mass densities. The first term is the Coulomb stress, the second a dielectrophoretic stress, attempting to pull regions of high permittivity into regions of low permittivity and the third is an electrostrictive stress. Strictly, equation 1.3 is only valid for fluids; a complex tensor treatment would be required in polymers, where shearing stresses are possible. Lewis notes that for PE at high fields, stresses parallel and perpendicular to the field are predicted to exist, expanding the structure, increasing the free volume level and generating microvoids. Since polyethylene chains have a negative electron affinity (Lewis discusses the fact that electrons travel through the inter- rather than the intra-chain regions) it is to be expected that these microvoids will then act as traps, altering the field distribution and completing the circle of electrical-mechanical-electrical interactions.

In summary, to obtain a thorough understanding of the dielectric breakdown properties of a given polymeric system, a comprehensive investigation of the thermal, mechanical, chemical and charge transport properties is required. Much uncertainty still surrounds even the simplest systems, such as polyethylene. On the other hand, a comprehensive understanding will be required of nanocomposite systems if their properties are to be optimised by design. In the search for new and improved nanocomposites, special attention should be paid to those materials whose behaviour can be explained simply, with a minimum of convoluted subsystems. On the other hand, if a material is developed with properties which are predictable from an empirical perspective but theoretically completely intractable, one must surely question the wisdom of commercialisation. With these considerations in mind, nanocomposites potentially have a distinct advantage over microcomposites: if near-uniform particle distributions can be easily obtained because of the volume exclusion effect, it is not unreasonable to anticipate the existence of many systems whose behaviour can be understood in terms of elegant interphase models with simple morphologies.

1.5 Aims and Objectives

As the field of nanocomposites remains immature, it is necessary to research their fundamental physical properties in parallel with studying their behaviour as appropriate engineering materials. Exhaustive comprehension of the complex interrelationships between these properties is unlikely to be immediately forthcoming. Nonetheless, such "twin-lens" research is invaluable in providing a foundation and defining more specific questions for future research. In the light of this, the aims of this work are twofold:

- To gain an understanding of the nature of the PE-MMT interactions via their effect on crystallisation kinetics and morphological evolution.

- To investigate the usefulness of PE-MMT nanocomposites as dielectric insulation materials, with particular consideration of their electrical breakdown behaviour.

The principal objective specific to the second aim was to use AC ramp breakdown testing of thin films between ball bearing electrodes. This technique is a rapid multi-modal failure test for characterising dielectric strength. As such, it is a good diagnostic tool for the pre-selection of materials for subsequent, application-specific testing.

Much research is still needed in the fields of nanocomposite preparation, quality control, physical understanding and empirical characterisation. Fortunately, in the case of MMT / thermoplastic systems, it is possible to largely circumvent the first of these by using masterbatch formulations. These consist of clay that has been thermodynamically compatibilised and dispersed into a matrix at a ~40% loading level by the supplier. This can then be let down into larger quantities of matrix by simple mechanical mixing techniques, making it possible to explore the above bullet points through variation of both the masterbatch chemistry and loading level. The first objective of this work is therefore to optimise the extrusion process and characterise the MMT dispersion in the extrudates.

It was decided to use a 90 : 10 w/w blend of LDPE : HDPE for the matrix. This method was used particularly in the morphological investigations of Norton and Keller [1.40] and it allows a useful modification of spherulite growth. Spherulite growth in pure HDPE involves the ejection of defective material and impurities to the edge of the spherulites, providing paths that are electrically and mechanically weak [1.31]. Conversely, lamellae of crystallising high density material can grow through an amorphous matrix, meaning that defective material remains essentially uniformly distributed throughout the material. This also provides a powerful contrast mechanism, with a suitable etching procedure, for electron microscopy and detailed morphological investigation. If used in conjunction with thermal analysis, much understanding can therefore be obtained about the nature of the PE-MMT interactions.

1.6 Contents of this thesis

Chapter 2 documents the optimisation of the extrusion process, together with characterisation of the extrudates in terms of LPE : BPE ratio, clay dispersion and degradation. It is essential in nanocomposites research that the compositions of the materials are reliably known. Chapters 3 and 4 then discuss the nature of the PE-MMT interactions as revealed via scanning electron microscopy (SEM) and thermal analysis of crystallisation and melting behaviour. Chapter 5 introduces the dielectric and mechanical properties of these materials, discussing parameters which are of paramount importance to an engineer: the AC dielectric loss, as probed by dielectric spectroscopy, and the Young's modulus (by tensile testing,) which limits the bend radius of a cable. On the other hand, relaxations are observed in dielectric spectroscopy and Dynamic Mechanical Thermal Analysis (DMTA) which can be interpreted directly in terms of fundamental molecular processes. Chapter 6 comprises a detailed investigation of the short term AC ramp breakdown behaviour of the materials. Finally, Chapter 7 assesses the conclusions of the previous chapters in the light of the aims and objectives discussed above, posing relevant questions for future research.